2013

Impact of Pre-Columbian Agriculture, Climate Change, and Tectonic Activity Inferred From a 5,700-Year Paleolimnological Record from Lake Nicaragua

Jennifer E. Slate
Northeastern Illinois University, j-slate@neiu.edu

Thomas C. Johnson
University of Minnesota - Duluth

Ted C. Moore
University of Michigan-Ann Arbor

Impact of pre-Columbian agriculture, climate change, and tectonic activity inferred from a 5700-year paleolimnological record from Lake Nicaragua

Jennifer E. Slate

Biology Department, Northeastern Illinois University, Chicago, IL 60625

e-mail: j-slate@neiu.edu

Thomas C. Johnson

Large Lakes Observatory and Department of Geological Sciences, University of Minnesota Duluth, Duluth, MN 55812

e-mail: tcj@d.umn.edu

Ted C. Moore

Department of Earth and Environmental Sciences, University of Michigan, Ann Arbor, MI 48109

e-mail: tedmoore@umich.edu

Key Words: Central America; Paleoclimate; Eutrophication; Diatoms; Tectonic activity; Lake depth

Abstract

Lake Nicaragua, the largest lake in Central America, is a promising site for paleolimnological study of past climate change, tectonic and volcanic activity, and pre-Columbian agriculture in the region. It is near the northern limit of the Intertropical Convergence Zone (ITCZ), which brings the rainy season to the tropics, so effects of decreasing precipitation due to southern migration of the ITCZ through the Holocene should be observable. Because fault zones and an active volcano lie within the lake, the long-term impact of tectonic and volcanic activity can also be examined. Finally, the fertile volcanic soils near the lake may have encouraged early agriculture. We analyzed diatoms, biogenic silica (BSi), total organic carbon (TOC), water content, volcanic glass, and magnetic susceptibility in a sediment core from Lake Nicaragua with eleven accelerator mass spectroscopy (AMS) radiocarbon dates, spanning ~5700 years. Sediment accumulation rates decreased from the bottom to the top of the core, indicating a general drying trend through the Holocene. An increase in eutrophic diatom abundance suggests that pre-Columbian agriculture impacted the lake as early as ~5400 cal yr BP. Above a horizon of coarser grains deposited sometime between ~5200-1600 cal yr BP, planktonic diatoms increased and remained dominant to the top of the core, indicating that water depth permanently increased. Although magnetic susceptibility peaked and water content dipped at the coarse horizon, volcanic glass fragments did not increase, suggesting that the coarse horizon and subsequent increase in water depth were caused by tectonic rather than by volcanic activity. Decreased accumulation rates of BSi and TOC indicate that water became clearer when depth increased.

Introduction

Relatively little paleolimnological data from Nicaragua have been published compared to elsewhere in Central America. Swain (1966) found diatoms and other potential indicators in the sediments of Lakes Nicaragua and Managua, but did not examine paleoenvironmental significance through time. Paleolimnological studies in Nicaragua have focused on the impact of a prehistoric hurricane on a Caribbean coastal forest (Urquhart 2009) and on the impact of humans versus climate on fire frequency during the past 1400 years (Avnery et al. 2011).

Paleoclimatological data from Nicaragua could inform us further on the history of climatic processes in Central America. For example, the Intertropical Convergence Zone (ITCZ), which is the convergence of northeast and southeast trade winds that brings summer rains to Central America and northern South America, has shifted substantially since the last glacial maximum. A trend toward increasingly drier climate in Central America through the Holocene, accentuated by an extremely dry period between 4500-3000 cal yr BP, has been attributed to southward migration of the average latitudinal position of the ITCZ (Haug et al. 2001; Mueller et al. 2009). Effects of southward ITCZ migration should be observable in paleoclimatic records from Nicaragua, which is near the northern limit of the ITCZ during Boreal summer.

Paleolimnological data from Nicaragua are also potentially informative about the spread of agriculture through Central America (Sandweiss 2007). Ometepe Island in Lake Nicaragua was settled by agriculturalists about 4000 years ago (Haberland 1986), but the beginning of indigenous agriculture in Nicaragua is not known. Humans cleared the landscape to cultivate

maize as early as 7000 cal yr BP in lowland central Panama (Dickau et al. 2007) but as late as 3000 cal yr BP in parts of northern Guatemala (Mueller et al. 2009).

Tectonic and volcanic events should be considered when constructing paleolimnological interpretations for Lake Nicaragua. For example, high sediment accumulation rates previously attributed to pre-Columbian agriculture in central Mexico may have actually been caused by tectonic activity (Israde-Alcántara et al. 2005). Former shorelines surrounding Lake Managua in Nicaragua indicate that the water level was previously 3 to 4 m higher, when large volcanic eruptions dammed the lake outlet (Cowen et al. 2002). Because Nicaragua lies along the active Central American volcanic front and has experienced numerous destructive earthquakes, it is an excellent location to study the impact of volcanic and tectonic activity.

With a surface area of almost 8000 km^2, Lake Nicaragua is the largest lake in Central America and supplies much of Nicaragua's water needs (Montenegro-Guillén 2003). To infer the impact of climate change, pre-Columbian human disturbance, and tectonic and volcanic activity, we analyzed a sediment core dated with eleven AMS radiocarbon dates spanning the past ~5700 years. We analyzed diatoms, biogenic silica, total organic carbon (TOC), water content, volcanic glass, and magnetic susceptibility in the core.

Study site

Lake Nicaragua (also known as Lake Cocibolca) is 7,585 km^2 in area and occupies a large portion of the southwest corner of the country (Fig. 1). Several fault zones lie within the graben lake, which formed in a tectonic depression (Funk et al. 2009). Lake Nicaragua also lies along the Central American volcanic front, which includes the active Concepción Volcano on Ometepe

Island in the lake. The lake lies at 31.4 m altitude with an average water temperature of 29^{o}C (Ahlgren et al. 2000). The large fetch (160 km) allows the water column (mean depth 13 m) to be mixed frequently by wind. The dry season is from December to April and the wet season from May to November, with rainfall in the catchment averaging 1200 mm yr^{-1} in the northwest and 4000 mm yr^{-1} in the southeast (Montenegro-Guillén 2003). Rainfall on the lake surface accounts for 46.1%, river inflow for 30.8%, ground water for 22.5%, and seepage outflow from nearby Lake Managua for 0.6% of the annual water budget (Montenegro-Guillén 2003). About 54% of water output is through the San Juan River, which empties into the Caribbean Sea, while the remaining output is through evaporation from the lake surface. The surrounding catchment is nearly three times the area of the lake, at 23,844 km^2 (Montenegro-Guillén 2003). Agriculture is extensive in the catchment, which has highly fertile, volcanic soils. Lake water has a pH of 7.5, Secchi depth averages 0.7 m, total phosphorus ranges from 20-80 μg L^{-1}, and total nitrogen averages 681 μg L^{-1} (Ahlgren et al. 2000). Phytoplankton biomass consists of 35% diatoms, 31% chlorophytes, 30% cyanobacteria, and 4% cryptophytes and dinoflagellates (Ahlgren et al. 2000).

Materials and methods

Core collection, magnetic susceptibility, and chronology

The 210-cm sediment core, designated LN97-14 LC, was collected on June 14, 1997 at a water depth of 9 m, using a gravity corer, at 11^{o}18.25'N and 85^{o}8.5'W (Fig. 1). Before the core was split, whole-core magnetic susceptibility was measured with a pass-through magnetometer, with

readings taken every 1 cm. The core was then split lengthwise, wrapped in plastic wrap, sealed in a d-tube, and stored at about 4°C. Accelerator Mass Spectrometry (AMS) ^{14}C dating was done on 11 bulk organic sediment samples (Table 1). Radiocarbon dates were corrected for $\delta^{13}C$, after which calibrated ages were calculated with CALIB 6.0 (http://calib.qub.ac.uk/calib/), using the INCAL09 calibration dataset. If a straight line could be drawn between the 2σ (95% probability) ranges for a group of sediment samples, then the linear sedimentation rate (LSR) between the samples was assumed to be constant and was calculated as the slope of that line. The midpoint of the depth range of each bulk sediment sample was used as the depth when calculating LSR.

Sediment carbon, biogenic silica, and water content

Sediment carbon, biogenic silica, and water content were measured in subsamples taken every 10 cm. Total carbon and inorganic carbon were determined by coulometry, and total organic carbon (TOC) was calculated by subtracting inorganic from total carbon content. Biogenic silica (BSi) was determined with a wet chemical digestion technique adapted from DeMaster (1979). Although this digestion method will also dissolve volcanic glass, sponge spicules, and phytoliths, those types of siliceous material were less abundant than diatoms, so BSi primarily represents diatom abundance. TOC and BSi are presented as % weight of the sediment and as mass accumulation rates (MAR). MAR was calculated with the formula $MAR = LSR * (1–\Phi) * \rho_{sed}$, where LSR = linear sedimentation rate, Φ = porosity, and ρ_{sed} = dry sediment density. Water content was determined by weighing the water-saturated sediment, freeze-drying, and weighing the dried sediment.

Diatoms and volcanic glass

Diatoms were analyzed in subsamples taken in 1-cm increments at every 5 cm throughout most of the core. Subsamples were freeze dried and organic matter was digested by heating in concentrated nitric acid and potassium dichromate. After repeated dilutions with distilled water to remove the acid, the solutions were dried onto glass coverslips in Battarbee trays (Battarbee 1973). The coverslips were mounted on glass microscope slides with Naphrax (refractive index of 1.7). Diatoms were identified to the lowest possible taxonomic level at 1000x with a Leica DMR microscope using Patrick and Reimer (1966, 1975), Kilham (1990), Stoermer and Andresen (1990), Krammer and Lange-Bertalot (1991-1997), Gasse et al. (2002) and Michels-Estrada (2003) as taxonomical references. Images of unidentified but common taxa were taken with a Leo model 435 VP scanning electron microscope. Five hundred diatom valves were identified and counted on a microscope slide from each subsample. Taxa that were $\geq$1% of diatom valves in at least one core section were analyzed with detrended correspondence analysis (DCA), detrending by segments, using Canoco for Windows version 4.02 (Jongman et al. 1995). DCA was used rather than correspondence analysis (CA) due to an arch effect with CA.

Taxa were placed into planktonic, benthic, and eutrophic categories based upon ecological information in references. Taxa were designated as primarily planktonic or benthic according to Rimet and Bouchez (2012) and Round (1990). *Aulacoseira ambigua* (Grun.) Simon*., Aulacoseira granulata* (Ehr.) Simon., *Belonastrum berolinensis* (Lemm.) Round & Maid*., Discotella stelligera* (Cleve & Grun.) Houk & Klee*, Navicula cryptotenella* Lange-Bert., and *Stephanodiscus minutulus* (Kütz.) Cleve & Möller were designated as eutrophic due to

characterization as eutrophic or highly eutrophic by van Dam et al. (1994) or Potapova and Charles (2007).

Volcanic glass fragments were counted in 200 fields of view on diatom slides from seven depth increments (2-3 cm, 37-38 cm, 67-68 cm, 144-115 cm, 129-130 cm, 159-160 cm, and 209-210 cm), using a Carl Zeiss petrographic polarizing microscope at 1000x magnification. Volcanic glass was identified by angular or vesicular shape, movement of the Becke line, and lack of interference colors in cross-polarized light (Enache and Cumming 2006). Three size categories of fragments were counted: 5-10 µm, 10-20 µm, and 20-30 µm. Fragments <5 µm were not counted and fragments >30 µm were not observed.

Results

Lithology and chronology

The entire core consists of a uniform, greenish-gray diatomaceous mud, with the exception of a slightly coarser horizon at ~68 cm. The coarse horizon is narrow (< 1 mm) but visible to the naked eye, appearing slightly darker than the rest of the core. Microscopic examination revealed that the coarse horizon consists of a slightly coarser diatomaceous mud. The grains were within the fine to medium sand size range and were a subangular to angular mix of quartz, feldspar, other silicate materials, and volcaniclastic grains. No sharp bedding contacts were observed.

The radiocarbon date at 204 cm, near the base of the 210-cm core, revealed that the core spans ~5700 cal yr BP (Table 1). Although radiocarbon dates increased downcore, a period of extremely slow sediment accumulation between 57-68 cm appears to represent a hiatus in the

record. The hiatus occurs directly above the coarse horizon at 68 cm depth and represents the interval between ~1600-5200 cal yr BP. With the exception of the depth interval of the hiatus, linear sedimentation rates increased downcore. The linear sedimentation rate was 0.037 cm yr^{-1} in the upper 33 cm of the core, 0.070 cm yr^{-1} between 33 and 58 cm, and 0.27 cm yr^{-1} between 67 and 204 cm (Fig. 2).

Diatoms

Throughout the core, diatoms were well-preserved and abundant, averaging 1.3 x 10^5 frustules mg^{-1} dry sediment. The majority of taxa were *Aulacoseira* or small Fragilariaceae (Fig. 4). *Aulacoseira* taxa included *A. agassizii* var. *malayensis* (Hust.) Simon, *A. ambigua*, and *A. granulata*. Unidentified *Aulacoseira* taxa were *A*. cf. *nyassensis* (O. Müll.) Simon and *A*. "sp. C" (Fig. 5). Small Fragilariaceae taxa included *Pseudostaurosira brevistriata* (Grun.) Will. & Round, *Staurosira construens* Ehr., *S. construens* var. *subsalina* (Hust.) Andres., Stoerm., & Kries, *Staurosira mercedes* Lange-Bert. & Rumr. and *Staurosirella pinnata* (Ehr.) Will. & Round. *D. stelligera*, *S. minutulus*, and *N. cryptotenella* were also common. Additional species occurred at lower abundances, such as *Nitzschia bacillum* Hust. and *Synedra delicatissima* W. Sm.

Detrended Correspondence Analysis (DCA) of the diatom data separated the core into three zones (Fig. 3). Axis 1 of the DCA separated zone A from the rest of the core and represented 48% of the total variation in the diatom data, indicating that zone A differed greatly from other zones. Zone A included all samples above the coarse horizon and hiatus, from 0–58 cm (modern to ~1600 cal yr BP). Zone A also included the sample at 62-63 cm from within the

hiatus, when sediment accumulation was extremely slow, but the sample was slightly apart from other samples in zone A and approached the position of zone B (Fig. 3). The uppermost three samples from 2-13 cm also plotted slightly apart from the rest of zone A.

Planktonic taxa increased but eutrophic taxa decreased in abundance in zone A (Fig. 4). Planktonic taxa were common in zones B and C, averaging 57.0% of all diatoms, but became dominant in zone A, averaging 92.0% of all diatoms. Although the eutrophic *D. stelligera* and *S. minutulus* increased in abundance, the overall abundance of eutrophic diatoms was lower in zone A than in any other zone. The species composition of *Aulacoseira* also changed in zone A, with *A. ambigua* and *A. granulata* decreasing in abundance (Fig. 4). Abundance of *A. ambigua* increased again in the uppermost samples of zone A.

Zones B and C were separated by axis 2 of the DCA, which represented an additional 8% of the total variation in the diatom data (Fig. 3). Zone B included all samples between 67–140 cm (~5160–5400 cal yr BP) and zone C included all samples between 144–210 cm (~5400–5690 cal yr BP). The overall abundance of eutrophic diatoms increased from an average of 42.6% in zone C to 46.4% in zone B, largely due to increased abundances of *D. stelligera* and *N. cryptotenella* (Fig. 4). *Nitzschia* cf. *modesta* Hust. (Fig. 5) also increased in zone B.

Geochemical, magnetic, and volcanic proxies

Magnetic susceptibility and water content were relatively constant throughout the core, with the exception of the coarse horizon at ~68 cm at the top of zone B (Fig. 6). At the coarse horizon, magnetic susceptibility increased to over 500 SI, more than 5-fold higher than the average of 92 SI throughout the rest of the core. Water content dipped to 70%, while remaining >80%

throughout the rest of the core. The spike in magnetic susceptibility and dip in water content did not indicate a tephra layer. Volcanic glass fragments were common at each depth analyzed but not more abundant in the coarse horizon (Fig. 6).

Mass accumulation rates of TOC and biogenic silica also changed at the coarse horizon (Fig. 6). Mass accumulation rates in zones B and C averaged 3.0 and 13.6 mg cm^{-2} yr^{-1} for TOC and biogenic silica, respectively. Above the coarse horizon, in zone A, the average accumulation rates of TOC and biogenic silica decreased nearly 10-fold, to 0.4 and 1.3 mg cm^{-2} yr^{-1}, respectively. Inorganic carbon was extremely low (<0.15%) throughout the entire core.

Discussion

The diatom community in zone C at the bottom of the core suggests a well-mixed, eutrophic lake. Codominance by *Aulacoseira* and small Fragilariaceae is common in polymictic subtropical or tropical lakes (Stoermer et al. 1992; Bradbury 2000; Haberyan and Horn 2005). *Aulacoseira* thrive with frequent mixing, which resuspends these heavily silicified diatoms into the water column (Kilham 1990). Small Fragilariaceae also thrive when sediments are frequently disturbed, probably because they are pioneer species (Stoermer et al. 1992). Mixing also brings nutrients from bottom sediments into the water column, favoring eutrophic species.

Although zone C was relatively eutrophic, the further increase in eutrophic diatoms in zone B suggests that pre-Columbian agriculture affected the lake as early as ~5400 cal yr BP. The two eutrophic taxa that increased the most in zone B, *D. stelligera* and *N. cryptotenella*, were identified as highly eutrophic by Potapova and Charles (2007), with N or P indicator values in the upper 25%. *Nitzschia* cf. *modesta* also increased in abundance, and the vast majority of

Nitzschia species indicate eutrophic water (van Dam et al. 1994; Potapova and Charles 2007). Eutrophic algae have increased in response to pre-Columbian agriculture in other paleolimnological studies. The eutrophic alga *Botryococcus* became common when pollen, geochemical, and magnetic data indicated that agriculture began at ~3800 cal yr BP near Hoya San Nicolas in central Mexico (Park et al. 2010). Similarly, eutrophic diatoms increased in Lago de Pátzcuaro in central Mexico when agriculture-related soil erosion intensified at ~1800 cal yr BP (Bradbury 2000).

Other aspects of the highly eutrophic taxa *D. stelligera* and *N. cryptotenella* are consistent with the hypothesis that agriculture-related landscape disturbance increased in zone B. *D. stelligera* increases after initial logging in a catchment, though it can decline again if deforestation or anthropogenic nutrient enrichment becomes severe (Köster et al. 2005). *N. cryptotenella* indicates moderate to high conductivity, which can result from landscape disturbance (Potapova and Charles 2003).

The inferred increase in eutrophication and landscape disturbance at ~5400 cal yr BP (95% probability range of 5310-5573 cal yr BP) is at about the same time that pre-Columbian agriculture intensified in many other areas of Central America. Forests were burned for *Zea* maize cultivation beginning ~5500 cal yr BP in Pacific Guatemala (Neff et al. 2006). Maize pollen first appeared at ~5400 cal yr BP in sediment cores from Belize and Honduras (Pohl et al. 1996, Rue et al. 2002). Pollen from weedy plants associated with agriculture began to increase at ~5000 cal yr BP in El Salvador (Dull 2004). Pollen from maize and disturbance taxa began to increase at ~4600 cal yr BP in the Mirador Basin of northern Guatemala (Wahl et al. 2006), although maize pollen did not appear until after 3000 cal yr BP elsewhere in northern Guatemala (Mueller et al. 2009).

In Lake Nicaragua, the inferred impacts of pre-Columbian agriculture at ~5400 cal yr BP are relatively moderate. Although the abundance of eutrophic diatoms increased, a large-scale change in diatom composition did not occur. Accumulation of sediment, TOC, and biogenic silica also did not increase measurably. Similarly, the impact of pre-Columbian agriculture was subtle in a Costa Rican lake. Instead of increasing total phosphorus, pre-Columbian agriculture changed the proportion of the mineral, organic, and occluded forms of phosphorus in lake sediments (Filippelli et al. 2010). Although the impact of early agriculture may have been diluted in a large lake such as Lake Nicaragua, the change in diatom composition shows that the base of the food chain was still affected. A change at the base of the food chain has larger implications due to the potential to affect higher trophic levels such as fish and turtles, which archaeological excavations show were an important food source for pre-Columbian populations along the shores of Lake Nicaragua (Haberland 1986).

More recent impacts are suggested by the slight separation of the uppermost samples between 2-13 cm from the rest of zone A. The eutrophic *A. ambigua* increased, but eutrophic diatoms as a whole did not increase and no patterns in the geochemical data were evident. Therefore, further research is necessary to determine the character and extent of recent impacts.

Unlike many other lakes, in which strong impacts of pre-Columbian agriculture masked signals of climate change, the moderate impacts to Lake Nicaragua allowed a signal of drying climate to be apparent. Decreasing sediment accumulation rates in zone A compared to the lower zones suggests that precipitation and runoff decreased in the late Holocene. Similarly, decreased precipitation and runoff through the Holocene was inferred in the Cariaco Basin off the northern coast of South America, hypothesized to be due to southward migration of the Intertropical Convergence Zone (ITCZ) (Haug et al. 2001). The ITCZ, which has a yearly north-

south migration that causes the characteristic wet and dry seasons in the tropics, also appears to adjust its average latitudinal position on a scale of thousands of years. Evidence of drying climate in Nicaragua, which is near the northern limit of the ITCZ, supports the argument that southward migration of the ITCZ from the mid to late Holocene caused widespread drying of the northern hemisphere tropics (Mueller et al. 2009).

Despite the drying climate, the diatom record clearly indicates that water depth increased above the coarse horizon and remained relatively deep to the present day. Planktonic diatoms became dominant in zone A, reflecting an increase in water depth that reduced the amount of light reaching the benthos, limiting benthic photosynthesis (Moos et al. 2005). In addition, *A. ambigua* and *A. granulata*, which are found at shallower depths in tropical African lakes, decreased in abundance (Kilham 1990). Although planktonics can become dominant in an assemblage without an increase in water depth if water clarity decreases, all of our evidence points towards water actually having become clearer in zone A. The percentage of eutrophic diatoms was lower in zone A than in any other zone. Mass accumulation rates of TOC and biogenic silica also decreased greatly, indicating decreased autogenic productivity. In addition, lower sediment accumulation rates suggest less suspended sediment in the water column.

The coarse horizon is not a distinct tephra layer. Volcanic glass fragments were not more abundant at the coarse horizon, but common throughout the core. Volcanic ash frequently erupts from the active Concepción Volcano on Ometepe Island within the lake, and volcaniclastic sediments within the catchment continuously erode into the lake (Swain 1966). Instead, the coarse horizon represents a subtle increase in abundance of sand, silt and tephra that indicates a high-energy depositional event. The coarser grain size appears to have caused the spike in magnetic susceptibility and dip in water content at the coarse horizon. Magnetic susceptibility

increases with grain size in sediments of primarily igneous origin (Dearing 1999). For example, magnetic susceptibility increased 4-fold in a coarse layer deposited by a tsunami off the coast of Portugal (Abrantes et al. 2005). Coarser, sandy deposits also have lower water content than clays, because smaller particles fill gaps between larger sand grains, decreasing the pore-to-solids ratio.

A likely cause of the coarse horizon and overlying hiatus is tectonic activity. Lake Nicaragua is in a very tectonically active region, close to the Mid-America convergence zone. Several fault zones occur within the lake (Funk et al. 2009), including the San Ramón Fault Zone near our coring site (Fig. 1). Tectonic activity can trigger large waves, or "tsunamis," within lakes that scour the lake bottom and leave a coarse deposit (Smoot et al. 2000; Israde-Alcántara et al. 2005; Freundt et al. 2007). After coarser particles winnow out and seiche activity dampens, finer grained material that had been eroded and mixed redeposits. As a result, the sediment directly overlying the coarse deposit would have apparently younger radiocarbon age, as occurs in our core directly above the coarse horizon at 68 cm.

The erosional event that caused the hiatus cannot be dated precisely because it may have compromised radiocarbon dates of bulk organic matter. The lowermost sample of zone A (62-63 cm) and the uppermost sample of zone B (67-68 cm) approach one another on the DCA graph, suggesting mixing within the hiatus between zones A and B (Fig. 3). The hiatus-causing erosional event did occur sometime between 5300-1600 cal yr BP and probably just prior to 1600 cal yr BP.

Water depth does not respond to changes in precipitation in an open lake such as Lake Nicaragua. Instead, the increase in water depth has to reflect a change in basin morphology that appears to be related to the coarse horizon and hiatus between zones A and B. The suspected

cause of the coarse horizon and hiatus, tectonic activity, can drastically alter lake morphology. For example, tectonic activity that caused a tsunami within Owens Lake in California also dropped one edge of the lake bottom (Smoot et al. 2000). Although volcanic activity is suspected to have triggered a prehistoric tsunami within Lake Nicaragua (Freundt et al. 2007), the relatively low number of volcanic glass fragments indicates that the coarse horizon in our core was not due to a volcanic eruption. Weather events such as a hurricane or large storm could also leave a coarse deposit, but are unlikely to cause long-term changes in lake depth. The possibility that tectonic activity deepened Lake Nicaragua supports the argument that geologic events must be considered when interpreting paleolimnological records of lake level change, especially in tectonically and volcanically active Mesoamerica (Israde-Alcántara et al. 2005).

Conclusions

Our multiproxy analysis of the longest paleolimnological record published thus far from Lake Nicaragua provides insights into the potential impact of pre-Columbian agriculture, climate change, and tectonic activity. The increase in eutrophic diatoms suggests that effects of agriculture were evident at ~5400 cal yr BP, about the same time that agriculture intensified throughout many areas of Central America. Because the inferred impacts of agriculture were relatively moderate in this large lake, a signal of drying climate could be detected, supporting the argument that southern migration of the ITCZ through the Holocene caused widespread drying in the northern hemisphere tropics (Mueller et al. 2009). Despite the drying climate, lake depth permanently increased sometime after ~5200 cal yr BP and probably just prior to ~1600 cal yr BP, apparently due to a change in basin morphology caused by tectonic activity. The possibility

that tectonic activity increased lake depth highlights the need to consider geologic events when interpreting paleolimnological records of lake level change.

Acknowledgements

We thank Jerry Urquhart for invaluable efforts to obtain the sediment core, Yvonne Chan for the geochemical data, and Kelly Burzic for counting volcanic glass fragments. Norm Andresen, Becky Bixby, Amy Bloom, Chris Donar, Mark Edlund, Kurt Haberyan, Matt Julius, Eduardo Morales, and Gene Stoermer provided helpful feedback about diatom identifications. Justin Funk kindly provided the bathymetric map of Lake Nicaragua. Isabelle Larocque and two anonymous reviewers provided helpful comments that improved the manuscript. This research was supported by NSF grant #9711788.

References

Abrantes F, Lebreiro S, Rodrigues T, Gil I, Bartels-Jónsdóttir H, Oliveira P, Kissel C, Grimalt JO (2005) Shallow-marine sediment cores record climate variability and earthquake activity off Lisbon (Portugal) for the last 2000 years. Quat Sci Rev 24: 2477-2494

Ahlgren I, Erikson R, Moreno L, Pacheco L, Montenegro-Guillén S, Vammen K (2000) Pelagic food web interactions in Lake Cocibolca, Nicaragua. Verh Internat Verein Limnol 27: 1740-1746

Avnery S, Dull RA, Keitt TH (2011) Human versus climatic influences on late-Holocene fire regimes in southwestern Nicaragua. Holocene 21: 699-706

Battarbee RW (1973) A new method for the estimation of absolute microfossil numbers, with reference especially to diatoms. Limnol Oceanogr 18: 647-653

Bradbury JP (2000) Limnologic history of Lago de Pátzcuaro, Michoacán, Mexico for the past 48,000 years: impacts of climate and man. Palaeogeogr Palaeoclimatol Palaeoecol 163: 69-95

Cowen H, Prentice C, Pantosti C, de Martini P, Strauch W (2002) Late Holocene earthquakes on the Aeropuerto Fault, Managua, Nicaragua. Bull Seismol Soc Am 92: 1694–1707

Dearing JA (1999) Holocene environmental change from magnetic proxies in lake sediments. In: Maher BA, Thompson R (eds) Quaternary Climates, Environments, and Magnetism. Cambridge Univ. Press, Cambridge, pp 231-278

DeMaster DJ (1979) The marine budgets of silica and ^{32}S. Ph.D. Thesis, Yale University

Dickau R, Ranere AJ, Cooke RG (2007) Starch grain evidence for the preceramic dispersals of maize and root crops into tropical dry and humid forests of Panama. Proc Natl Acad Sci USA 104: 3651-3656

Dull RA (2004) An 8000-year record of vegetation, climate, and human disturbance

from the Sierra de Apaneca, El Salvador. Quat Res 61: 159-167

Enache MD, Cumming BF (2006) The morphological and optical properties of volcanic glass: a tool to assess density-induced vertical migration of tephra in sediment cores. J Paleolimnol 35: 661-667

Filippelli GM, Souch C, Horn, SP, Newkirk, D (2010) The pre-Columbian footprint on terrestrial nutrient cycling in Costa Rica: insights from phosphorus in a lake sediment record. J Paleolimnol 43: 843-856.

Freundt A, Strauch W, Kutterolf S, Schmincke HU (2007) Volcanogenic tsunamis in lakes: examples from Nicaragua and general implications. Pure Appl Geophys 164: 527-545

Funk J, Mann P, McIntosh KD, Stephens J (2009) Cenozoic tectonics of the Nicaraguan depression, Nicaragua, and Median trough, El Salvador, based on seismic-reflection profiling and remote-sensing data. Geol Soc Am Bull 121:1491-1521

Gasse F, Barker P, Johnson TC (2002) A 24,000 yr diatom record from the northern basin of Lake Malawi. In: Odada EO, Olago DO (eds) The East African Great Lakes: Limnology, Paleolimnology and Biodiversity. Kluwar, Netherlands, pp 393-414

Haberland W (1986) Settlement patterns and cultural history of Ometepe Island, Nicaragua: A preliminary sketch. In: Lange FW, Norr L (eds) Prehistoric Settlement Patterns of Costa Rica. Steward Anthropological Society, Urbana, Illinois, pp 369-386

Haberyan KA, Horn SP (2005) Diatom paleoecology of Laguna Zoncho, Costa Rica. J Paleolimnol 33: 361-369

Haug GH, Hughen KA, Sigman DM, Peterson LC, Röhl U (2001) Southward migration of the Intertropical Convergence Zone through the Holocene. Science 293: 1304-1308

Israde-Alcántara I, Garduño-Monroy VH, Fisher CT, Pollard HP, Rodríguez-Pascua MA (2005) Lake level change, climate, and the impact of natural events: the role of seismic and volcanic events in the formation of the Lake Patzcuaro Basin, Michoacan, Mexico. Quat Int 135: 35-46

Jongman RHG, ter Braak CJF, van Tongeren OFR (1995) Data analysis in community and landscape ecology. Cambridge University Press, Cambridge, UK

Kilham P (1990) Ecology of *Melosira* species in the Great Lakes of Africa. In: Tilzer MM, Serruya C (eds) Large Lakes: Ecological Structure and Function. Springer-Verlag, Berlin, pp 414-427

Köster D, Pienitz R, Wolfe BB, Barry S, Foster DR, Dixit SS (2005) Paleolimnological assessment of human-induced impacts on Walden Pond (Massachusetts, USA) using diatoms and stable isotopes. Aquat Ecosyst Health Manag 8: 117-131

Krammer K, Lange-Bertalot H (1991-1997) Bacillariophyceae. In: Ettl H, Gerloff J, Heynig H, Mollenhauer D (eds) Süβwasserflora von Mitteleuropa. Vol. 2/1-4. Gustav Fischer Verlag, Stuttgart/Jena

Michels-Estrada A (2003) Ökologie und Verbreitung von Kieselalgen in Fließgewässern Costa Ricas als Grundlage für eine biologische Gewässergütebeurteilung in den Tropen. [Ecology and distribution of diatoms in rivers of Costa Rica as a basis for biological water quality assessment in the tropics] In: Dissertationes Botanicae, Band 377. J. Cramer, Berlin, pp 1-244

Montenegro-Guillén S (2003) Lake Cocibolca/Nicaragua. In: Lake Basin Management Initiative: Experience and Lessons Learned Brief. St. Michael's College, Vermont, pp 1-29

Moos MT, Laird KR, Cumming, BF (2005) Diatom assemblages and water depth in Lake 239 (Experimental Lakes Area, Ontario): implications for paleoclimatic studies. J Paleolimnol 34: 217-227

Mueller AD, Islebe GA, Hillesheim MB, Grzesik DA, Anselmetti FS, Ariztegui D, Brenner M, Curtis JH, Hodell DA, Venz, KA (2009) Climate drying and associated forest decline in the lowlands of northern Guatemala during the late Holocene. Quat Res 71: 133-141

Neff H, Pearsall DM, Jones JG, Arroyo B, Collins SK, Freidel DE (2006) Early Maya adaptive patterns: Mid-late Holocene paleoenvironmental evidence from Pacific Guatemala. Latin Am Antiquity 17: 287-315

Park J, Byrne R, Böhnel H, Molina Garza R, Conserva M (2010) Holocene climate change and human impact, central Mexico: a record based on maar lake pollen and sediment chemistry. Quat Sci Rev 29: 618-632

Patrick R, Reimer CW (1966, 1975) The diatoms of the United States. Vol. 1-2. Monographs of the Academy of Natural Sciences of Philadelphia, No. 13

Pohl MD, Pope KO, Jones JG, Jacob JS, Piperno DR, deFrance SD, Lentz DL, Gifford JA, Danforth ME, and Josserand JK (1996) Early agriculture in the Maya lowlands. Latin Am Antiquity 7: 355-372

Potapova M, Charles DF (2003) Distribution of benthic diatoms in U.S. rivers in relation to conductivity and ionic composition. Freshw Biol 48: 1311–1328

Potapova M, Charles DF (2007) Diatom metrics for monitoring eutrophication in rivers of the United States. Ecol Indicators 7: 48-70

Rimet F, Bouchez A (2012) Life-forms, cell-sizes and ecological guilds of diatoms in European rivers. Knowledge Manag Aquat Ecosyst 406: 1-14

Round FE, Crawford RM, Mann DG (1990) The Diatoms. Cambridge, New York

Rue D, Webster D, Traverse A (2002) Late Holocene fire and agriculture in the Copan Valley, Honduras. Ancient Mesoam 13: 267-272

Sandweiss DH (2007) Small is big: the microfossil perspective on human-plant interaction. Proc Natl Acad Sci USA 104: 3021-3022

Smoot JP, Litwin RJ, Bischoff JL, Lund SJ (2000) Sedimentary record of the 1872 earthquake and “tsunami” at Owens Lake, southeast California. Sediment Geol 135: 241–254

Stoermer EF, Andresen NA (1990) *Aulacoseira agassizii* in North America. Beiheft zur Nova Hedwigia 100: 217-223

Stoermer EF, Andresen NA, Schelske CL (1992) Diatom succession in the recent studies of Lake Okeechobee, Florida, U.S.A. Diatom Res 7: 367-386

Swain FM (1966) Bottom sediments of Lake Nicaragua and Lake Managua, western Nicaragua. J Sediment Petrol 36: 522-540

Urquhart GR (2009) Paleoecological record of hurricane disturbance and forest regeneration in Nicaragua. Quat Int 195: 88-97

van Dam H, Mertens A, Sinkeldam J (1994) A coded checklist and ecological indicator values of freshwater diatoms from the Netherlands. Neth J Aquat Ecol 28: 117-133

Wahl D, Byrne R, Schreiner T, Hansen R (2006) Holocene vegetation change in the northern Petén and its implications for Maya prehistory. Quat Res 65: 380-389

Table 1 AMS Radiocarbon dates of bulk sediment samples

Lab number*	Depth (cm)	‰ $\delta^{13}C$	^{14}C year BP**	Cal. year BP^{+}	Range^{++}
OS 15665	4	-23.07	>Modern	N/A	N/A
Beta 212598	11-14	-23.1	740 ± 40	684	569 – 735
Beta 212597	21-24	-22.3	1040 ± 40	955	804 – 1057
Beta 167866	32-33	-21.8	1290 ± 40	1229	1093 – 1297
Beta 167867	57-58	-20.3	1680 ± 40	1588	1446 – 1704
Beta 167868	62-63	-19.5	2660 ± 40	2774	2739 – 2849
Beta 155704	67-68	-18.0	4500 ± 40	5163	4980 – 5305
Beta 155705	102-103	-19.0	4700 ± 40	5413	5319 – 5580
Beta 155706	139-140	-18.9	4660 ± 40	5403	5310 – 5573
Beta 155707	174-175	-18.0	4830 ± 40	5545	5473 – 5647
OS 15670	204	-18.77	4960 ± 45	5689	5598 – 5877

*OS=Woods Hole Oceanographic Institution; Beta=Beta Analytic, Inc.
** Corrected for $\delta^{13}C$
$^{+}$ median probability
$^{++}$ 2σ range (95% probability) of calibrated year BP

Figure 1. Coring site on bathymetric map of Lake Nicaragua (modified from Funk et al. 2009). Each contour line represents 1 m. The main fault zones in the lake are the Jesus Maria fault zone (JMFZ), the San Ramón fault zone (SRFZ), and the Morrito fault zone (MFZ). Inset: Location of Lake Nicaragua relative to Central America and northern South America.

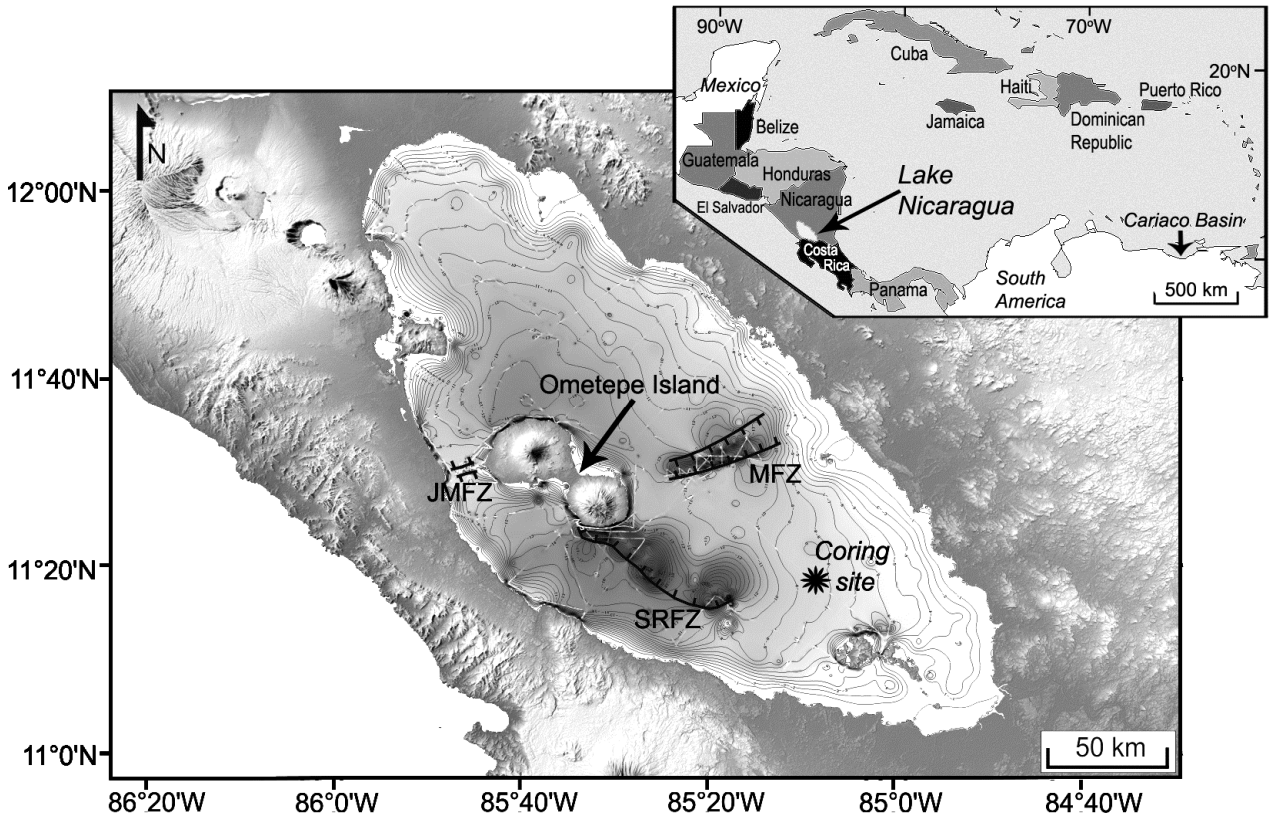

Figure 2. AMS radiocarbon dates of bulk sediment samples vs. depth. Black circles indicate median probability of calibrated dates and error bars indicate 2σ ranges. Linear sedimentation rates (cm yr^{-1}) are also provided.

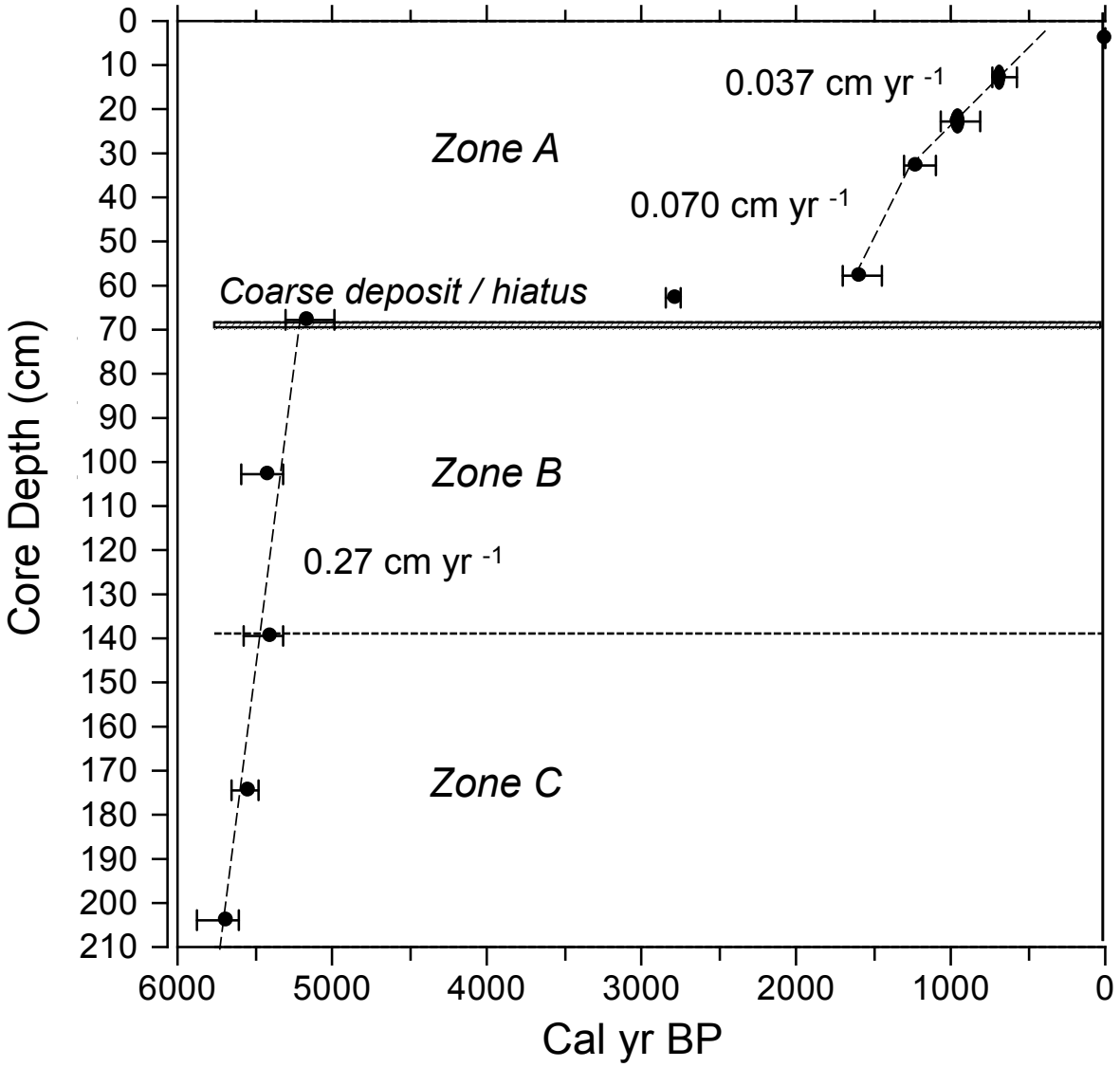

Figure 3. Detrended correspondence analysis of diatom data. Samples with similar taxa composition lie close to one another on the ordination graph, while less similar samples are farther apart.

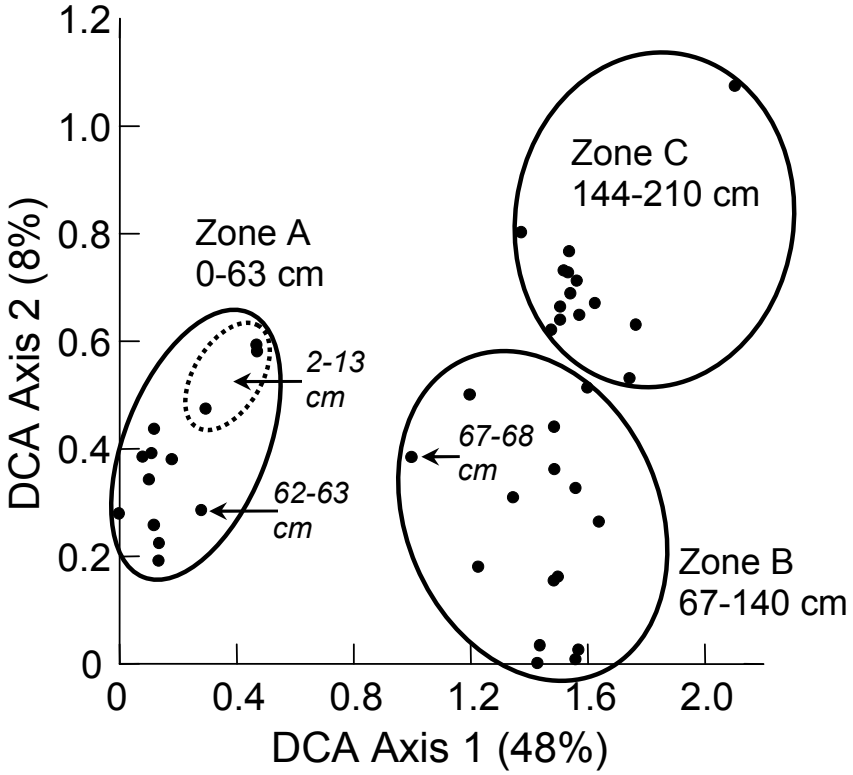

Figure 4. Relative abundances of diatom taxa that were ≥1% of all diatoms in at least one core section. The x-axis scale of each individual taxon begins with 0%. Eutrophic taxa have an asterisk after the taxon name. Total percentages of all planktonic taxa and all eutrophic taxa are also provided. Zones (as determined by detrended correspondence analysis of diatom data) and median calibrated radiocarbon dates are indicated.

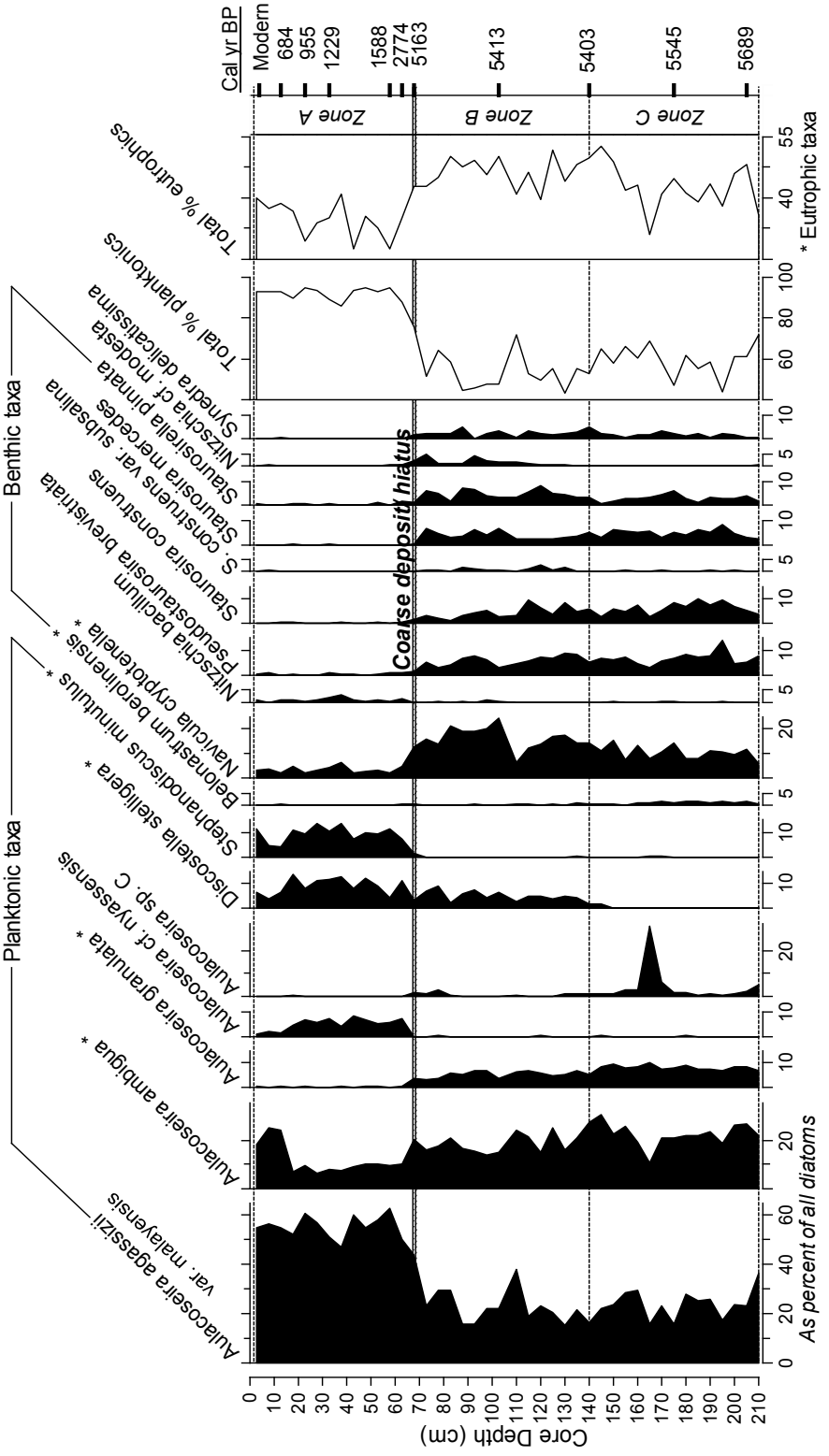

Figure 5. Scanning electron microscope images of unidentified diatom taxa. A. *Aulacoseira* "sp. C." B. Closer view of areolae of *Aulacoseira* "sp. C." C. *Aulacoseira* cf. *nyassensis*. D. Closer view of areolae of *Aulacoseira* cf. *nyassensis*. E. *Nitzschia* cf. *modesta*.

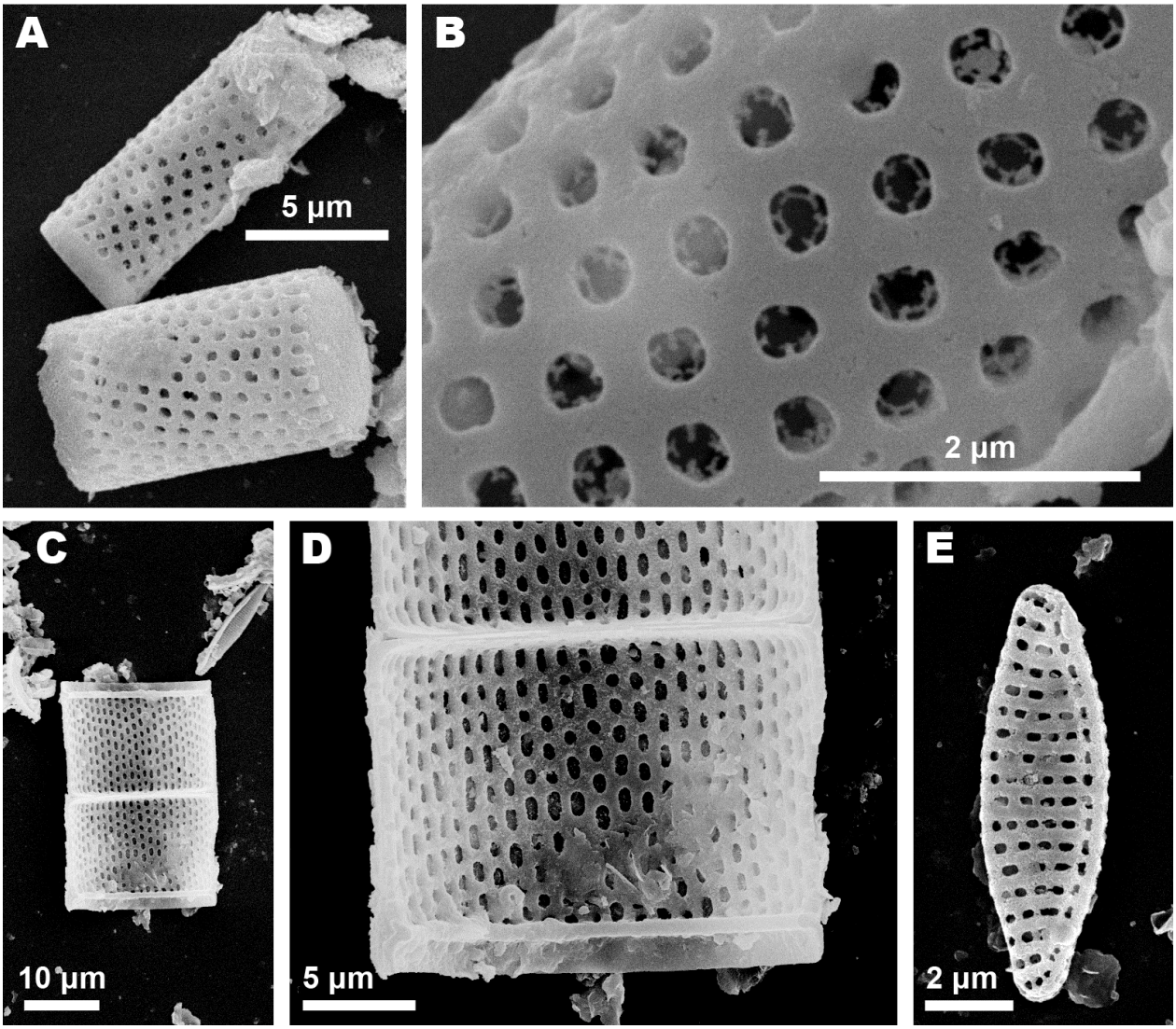

Figure 6. Stratigraphy of magnetic susceptibility, water content, total organic carbon (TOC), biogenic silica, and volcanic glass fragments.